On the Origins of the Hydrophobic Effect: Observations from Simulations of *n*-Dodecane in Model Solvents

A. Wallqvist and D. G. Covell
Frederick Cancer Research and Development Center, National Cancer Institute, Science Applications International Corporation, Frederick, Maryland 21702 USA

ABSTRACT The importance of the small size of a water molecule as contributing to the hydrophobic effect is examined from simulations of *n*-dodecane in different solvents. The earlier observations of the origin of hydrophobicity, derived from cavity formations by Pratt and Pohorille (1992, *Proc. Natl. Acad. Sci. USA.* 89:2995–2999) and Madan and Lee (1994, *Biophys. Chem.* 51:279–289), are shown to be largely consistent for a hydrocarbon-induced water pocket. In effect, the small size of a water molecule limits the probability (and hence free energy) of finding an appropriate void in the fluid that will accommodate a solute. In this work a simulated collapse of an *n*-dodecane molecule in H_2O, CCl_4, and a water-like Lennard-Jones solvent indicates that the induced entropy and enthalpy changes are qualitatively similar for hydrogen-bonded and Lennard-Jones water solvents. These results suggest that a large part of the hydrophobic response of solutes in aqueous solutions is due to the small size of the solvent. Important quantitative differences between the studied water solvents indicate that the hydrogen-bonded properties for water are still needed to determine the overall hydrophobic response.

INTRODUCTION

Nonpolar molecules are not readily soluble in water. This hydrophobic property is also considered an important contribution to the microscopic forces responsible for assembling biomolecular aggregates, such as membranes and proteins (Kauzmann, 1959; Tanford, 1973; Ben-Naim, 1974; Franks, 1975; Chan et al., 1979; Dill, 1990; Blokzijl and Engberts, 1993). Experimental quantification of the hydrophobic effect has been derived mainly from careful measurement of the solvation properties of small nonpolar molecules, such as rare gas atoms and methane in water (Crovetto et al., 1982). From such measurements we know that the desolvation of hydrophobic surfaces is accompanied by a significant release of entropy associated with the surface waters. This has traditionally been interpreted as an order/disorder phenomenon. Water molecules at a solute interface are more "structured"—forming a regular network of ordered waters—than water molecules in the bulk; thus the withdrawal of exposed hydrophobic surfaces will result in a free-energy gain stemming from a large $-T\Delta S$ contribution. Although this picture of waters in contact with hydrophobic surfaces may be suggestive of outright clathrate structures (Sloan, 1990), the many simulations of water/hydrophobic systems over the years have not supported such a picture. Arguments based solely on the concept of "water structure" have a tendency to be inherently ambiguous and devoid of substantial content (Holtzer and Emerson, 1969) and should be cautiously applied. Rather minute changes in structural as well as hydrogen bond properties have instead been reported (Blokzijl and Engberts, 1993). The lack of gross structural changes is, however, not inconsistent with the entropic nature of hydrophobic association (Smith et al., 1992; Smith and Haymet, 1993).

The hydrophobic effect has naturally attracted great interest among theoreticians. Scaled particle theory (Reiss, 1965; Stillinger, 1973) can describe the solvation of nonpolar solutes. The integral equation theory of the hydrophobic effect by Pratt and Chandler (1977, 1980) is highly successful in accounting for both structural and thermodynamic properties of dilute solutions of apolar molecules. Yet none of these theoretical treatments explicitly include any structural details of the hydration shell; indeed, an explicit approximation in the Pratt/Chandler work is that solvent does not restructure itself around solutes.

Detailed treatments of a solute/solvent system may be achieved by Monte Carlo and molecular dynamics simulation techniques. Provided the underlying potential surfaces are realistic, these statistical mechanical tools can provide accurate measures of both structural and thermodynamic properties of model systems. Simulation studies have focused on the hydrophobic attraction in simplified model systems, e.g., apolar dimers and the conformational equilibrium of butane in water (Blokzijl and Engberts, 1993). An important aspect of this theoretical work is the recognition that solute pairing can be unfavorable compared to a solvent-separated solute pair. This result was first recognized by Pratt and Chandler, and later confirmed by computer simulations employing explicit molecular models of water (Pangali et al., 1979a,b). Inclusion of more refined potential functions containing a self-consistent polarizability support the same picture (New and Berne, 1995). Theoretical studies of *n*-butane in both polar and nonpolar solvents have displayed a greater variety of results (Pratt and Chandler, 1977; Rebertus et al., 1979; Pratt et al., 1980; Rosenberg et al., 1982; Jorgensen, 1982; Zichi and Rossky, 1986; Tobias and Brooks, 1990). The presence of a *gauche*

Received for publication 3 November 1995 and in final form 7 May 1996.
Address reprint requests to Dr. A. Wallqvist, NCI-FCRDC-SAIC, P.O. Box B, Frederick, MD 21702. Tel.: 301-846-5396; Fax: 301-846-1116; E-mail: wallqvis@ncifcrf.gov.

0006-3495/96/08/600/09 $2.00

state has been found to be negligible or only slightly more favorable than the *trans* state. The variability of these results may stem from the difference in simulation and interaction parameters of the model systems under investigation.

The concept of the low solubility of nonpolar solutes in water as being ultimately a consequence of the molecular size of water has long been considered from thermodynamic arguments (Eley, 1939a,b; Lee, 1985). The agreement with the simulation data of both scaled particle and integral equation theories prompted Pohorille and Pratt (1990, 1992) to focus on the unifying aspects common to the theoretical treatment of the model liquid. As the solubility of small solute molecules depends largely on the work required to form a suitable cavity in the solvent (Ben-Naim, 1974), these studies focused on naturally occurring, transient cavities for a number of solvents. The outstanding property of water that is absent in hydrocarbon solvents is its ability to partition the unoccupied volume into smaller packets than for an alkane solvent. Even though this "free" volume is roughly the same for water and hydrocarbon liquids, the probability of finding a sufficiently large cavity to accommodate a solute in water is thus smaller, and hence solvation of a small solute carries a heavier free-energy penalty in water than in liquid alkanes. In the work of Madan and Lee (1994) the free-energy cost of forming a cavity of a given size was shown to be roughly the same in a "water" liquid stripped of hydrogen bond capabilities, but with the same molecular volume (i.e., retaining the same Lennard-Jones parameters), as in a conventionally modeled liquid water. The size of the water molecule and its resultant ability to effectively fill voids is to a large part responsible for the hydrophobic effect. This effect is naturally included in both the scaled particle theory and the integral equation treatment of aqueous solutions. Experimentally, solvophobic effects have also been observed for liquids other than water, e.g., long-range "hydration" forces between hydrophobic plates are observed in ethylene glycol (Tsao et al., 1993). Molecular size has also been shown to determine the decay length of the long-range forces between neutral lipid bilayers in water (Leikin et al., 1993).

In a previous paper (Wallqvist and Covell, 1995) we investigated the influence of solvent waters on the conformational equilibrium of a single solvated *n*-dodecane molecule. Even though an extended state of this molecule corresponds to the most probable conformation in solution, it was possible to monitor the entire free-energy contribution of the solvent while contracting an initially fully extended chain into a compact conformation. Compact states minimize the exposed solute/solvent interface; however, it is the balance between the solvent and intramolecular contributions from the solute that determines the overall conformational equilibrium. In the current work we reexamine the premises regarding the importance of solvent size for the hydrophobic effect by comparing the results of water simulations with new data from studies employing nonaqueous solvents. In contrast to earlier studies of naturally occurring cavities in liquids, we study cavities that are induced by the solute itself, arising from conformational changes of the solute. It can be argued that if a solute imparts special ordering of neighboring waters not present in the naturally occurring voids of the liquid, studies of spontaneous cavities may be irrelevant. We avoid this problem here by having the large solute molecule occupy a volume greater than any naturally occurring cavity in liquid water.

To begin, we describe the computational approach to the problem and outline the technical details of the simulations and calculations involved in determining the free energy change of an *n*-dodecane molecule in solution. The latter part of the paper describes properties of the different solvents and the free-energy contributions to bending the hydrocarbon chain in solution.

COMPUTATIONAL STRATEGIES

Ideally we would like to characterize the entire free-energy surface of *n*-dodecane, encompassing all conformational states, in a solvent. From such a hypersurface we could immediately determine those configurations favored by a certain solvent, as well as the relative importance of compact and extended states. In principle, such calculations are possible from molecular dynamics simulations, although the computer times required make these calculations infeasible. The approach used here is based on limiting the configurational search to those states that are most probable when contracting the chain from an initial extended all-*trans* state to a compact state. In contrast to a very long chain of hundreds of monomers, a single *n*-dodecane is not expected to form an outright separate phase where parts of the chain are solvated by surrounding chain segments. This condition permits the unique opportunity to follow a single coordinate, namely the end-to-end distance, r_{ee}, as a measure of compactness of the chain. The end-to-end distance is measured as

$$r_{ee} = \left| \mathbf{r}_1 - \mathbf{r}_N \right|, \qquad (1)$$

where $\mathbf{r}_{1,N}$ denotes the coordinates of the endgroups on the *n*-dodecane molecule. By introducing small perturbations in the end-to-end distance, a free-energy difference can then be calculated and used to gauge the relative importance of different conformational states. This approach was verified in the previous calculations of *n*-dodecane in gas phase and applied to a dense water system (Wallqvist and Covell, 1995). Here, we investigate two new solvents and contrast the results with those obtained from a liquid water solvent. Thus, we study a nonpolar carbon tetrachloride-like fluid as well as a water-mimicking single-site Lennard-Jones (LJ) solute, designed to give the same volume characteristics as liquid water at room temperature.

Model interactions

Molecular interactions are based on a pairwise additive description of the intermolecular potential surfaces. A fur-

TABLE 1 Solvent interaction parameters

Solvent LJ potential

Atom *i*/atom *j*	A_{ij}^{12} (10^7 Å^{12} kJ/mol)	C_{ij}^{6} (10^3 Å^6 kJ/mol)
$C(CCl_4)/C(CCl_4)$	566.6	264.5
$O(LJ\text{-}H_2O)/O(LJ\text{-}H_2O)$	1.161	3.353

RER-water interaction parameters

q_O (*e*)	q_H (*e*)	C_{12} (kJ/mol Å^{12})	C_6 (kJ/mol Å^6)	C_4 (kJ/mol Å^4)	C_t (kJ/mol)	w_t (Å^{-2})	r_t (Å)
−0.920	0.460	3,500,000	−3,100	15.0	−1.000	1.5	4.5

ther simplification for the non-hydrogen-bonded molecules is that only the heavy atoms are modeled explicitly, i.e., a unified atom approach.

The carbon tetrachloride molecule was modeled as a single-site Lennard-Jones solvent, with the intermolecular interaction between CCl_4 molecules *i* and *j* given by

$$V_{ij}^{LJ}(r_{ij}) = \frac{A_{ij}^{12}}{r_{ij}^{12}} - \frac{C_{ij}^{6}}{r_{ij}^{6}}, \tag{2}$$

where r_{ij} denotes the interatomic distance, and A^{12} and C^6 coefficients are listed in Table 1 and correspond to the values of Tobias and Brooks (1990). The realism of modeling the CCl_4 liquid as a five-atom molecule is lost, although the overall effect of a large, roughly spherical hydrophobic solvent is retained.

The numerous models of liquid water used for molecular simulations are basically constructed using a combination of van der Waals and electric dipolar forces. To isolate the issues regarding molecular "size," a simplified water construction was used where the van der Waals interactions were modified to give a liquid with the same size and density as real liquid water at 300 K and 1 atm, but without any dipolar contributions. This "molecule" has only one site, corresponding to an oxygen atom, and neglects hydrogen sites. There are no electrostatic interactions between these LJ waters. This is similar to the simplified water used by Pratt and Pohorille (1992). The interaction coefficients used in this simulation are given in Table 1.

The aqueous environment used as a reference for comparison of free-energy differences was previously modeled by the RER(pair) potential (Wallqvist and Berne, 1993). In this scheme the water molecules are represented as rigid three-site entities. The monomer geometry of a water molecule is given by a bond length $r_0 = 0.96$ Å and a bond angle $\theta_0 = 104.52°$. Partial charges assigned to the oxygen and hydrogen atoms yield an effective permanent dipole moment of 2.60 D. The functional form of this potential is given by

$$V_{pair}(\{\mathbf{R}_i\},\{\mathbf{R}_j\}) = \frac{C_{12}}{r_{oo}^{12}} + \frac{C_6}{r_{oo}^{6}} + \frac{C_4}{r_{oo}^{4}} + C_t e^{-w_t(r_{oo}-r_t)^2} + \sum_{\alpha\epsilon i,\beta\epsilon j}^{atoms} \frac{q_\alpha q_\beta}{4\pi\epsilon_0 r_{\alpha\beta}}, \tag{3}$$

where $\{\mathbf{R}_i\}$ denotes the coordinates of water molecule *i*, r_{oo} is the distance between oxygen atoms on water *i* and *j*, and $r_{\alpha\beta}$ is the radial distance between two atoms on the *i*th and *j*th water molecules. The parameter values for the model are given in Table 1. In contrast to many conventional models of dipolar fluids, this model has been parameterized to take into account the potential energy cost of creating the effective dipole moment (Berendsen et al., 1987; Watanabe and Klein, 1989; Wallqvist and Berne, 1993).

The *n*-dodecane molecule was modeled as a set of connected CH_3- or -CH_2- units. The hydrocarbon chain dynamics are modeled via bond-angle bending and torsional motion. Bond vibrations are suppressed by fixing the bond length to 1.53 Å. Bond-angle motions are included as bond-bending and dihedral angle rotations are coupled. A harmonic bond-bending term between three connected methylene units forming an angle θ is thus used,

$$V_\theta(\mathbf{r}_i,\mathbf{r}_j,\mathbf{r}_k) = \frac{1}{2}k_\theta(\theta_o - \theta)^2, \tag{4}$$

where k_θ is the harmonic force constant, and θ_0 is the equilibrium bond angle. Parameter values are those of Weiner et al. (1984) and are given in Table 2. The dihedral potential was taken from the work of Jorgensen (Jorgensen et al., 1984) and is represented as a truncated Fourier series,

$$V_\phi(\mathbf{r}_i,\mathbf{r}_j,\mathbf{r}_k,\mathbf{r}_l) = V_0 + V_1\cos\phi + V_2\cos 2\phi + V_3\cos 3\phi, \tag{5}$$

where ϕ is the dihedral angle between the connected methylene units, $\mathbf{r}_i$, $\mathbf{r}_j$, $\mathbf{r}_k$, and $\mathbf{r}_l$. The coefficients are summarized in Table 2. Intramolecular interactions between methylene units that are separated by four or more bonds utilize a Lennard-Jones potential (Eq. 2) with the parameters given in Table 2 (Jorgensen et al., 1984; Harris, 1992).

Only the heavy atom of solvent molecules interacts with the methyl and methylene units in the *n*-dodecane molecule via the Lennard-Jones interaction of Eq. 2 and with coefficients given in Table 3 (Jorgensen et al., 1984). The LJ waters utilize the same intermolecular potential as RER water for interactions with the hydro-

TABLE 2 Hydrocarbon interaction parameters

Dihedral potential	
V^0	9.74 kJ/mol
V_1	2.95 kJ/mol
V_2	−0.57 kJ/mol
V_3	6.58 kJ/mol
Bending potential	
k_θ	527.2 kJ/mol/rad^2
θ_0	1.962 rad

Intramolecular LJ potential

Atom *i*/atom *j*	A_{ij}^{12} (10^7 Å^{12} kJ/mol)	C_{ij}^{6} (10^3 Å^6 kJ/mol)
CH_3/CH_3	3.682	10.385
CH_2/CH_3	2.483	7.004
CH_2/CH_2	3.023	8.527

TABLE 3 Solvent/hydrocarbon interaction parameters

Solvent-hydrocarbon LJ potential Atom *i*/atom *j*	A_{ij}^{12} (10^7 Å^{12} kJ/mol)	C_{ij}^{6} (10^3 Å^6 kJ/mol)
O(RER(pair)-H_2O)/CH_3	0.961	5.146
O(RER(pair)-H_2O)/CH_2	0.789	4.226
O(LJ-H_2O)/CH_3	0.961	5.146
O(LJ-H_2O)/CH_2	0.789	4.226
C(CCl_4)/CH_3	11.44	13.38
C(CCl_4)/CH_2	11.38	11.38

carbon molecules. The CCl_4/dodecane parameters were taken from the work of Tobias and Brooks (1990); they are given in Table 3.

Free-energy estimates

The free-energy difference between two differently constrained hydrocarbon chains in a solvent can be calculated from statistical perturbation theory (Beveridge and DiCapua, 1989) by performing an ensemble average of the perturbed system using configurations from the unperturbed system. Provided the decrease in end-to-end separation, r_{ee}, proceeds in sufficiently small steps, the entire free-energy curve can be calculated. Thus, the change in Helmholtz free energy between two systems, r_{ee}^0 and r_{ee}^1, containing N particles at a given temperature, T, and volume is given by (Beveridge and DiCapua, 1989)

$$\Delta A = A(r_{ee}^1) - A(r_{ee}^0) = -kT \ln\langle e^{-[V(r_{ee}^1)-V(r_{ee}^0)]/kT}\rangle_0, \quad (6)$$

where k is Boltzmann's constant, V is the total potential energy, and the brackets indicate an ensemble average of the exponential of perturbation in the reference system.

Although associated with a larger sampling problem, the entropy contribution to the free-energy change in the perturbed system can likewise be evaluated from the temperature derivative of the Helmholtz free energy as (Postma et al., 1982; Smith and Haymet, 1993)

$$-T\Delta S = \Delta A - \frac{\langle \mathcal{H}_1 e^{-\Delta V/kT}\rangle_0}{\langle e^{-\Delta V/kT}\rangle_0} + \langle \mathcal{H}_0\rangle_0, \quad (7)$$

where $\mathcal{H}_1$ and $\mathcal{H}_0$ are the perturbed and the reference Hamiltonians, respectively.

Simulation parameters

To accommodate the most extended hydrocarbon conformation, a periodically replicated cubic box of 21,718 Å^3 was used together with 717 simplified LJ waters. Only one *n*-dodecane molecule was solvated, in essence corresponding to an infinitely dilute solution. In the carbon tetrachloride simulations, 211 solvent particles enclosed one hydrocarbon chain in a 34,581 Å^3 unit cell.

The equations of motions were integrated using the Rattle version (Andersen, 1983) of the velocity Verlet algorithm (Swope et al., 1982) to maintain the internal bond lengths of the hydrocarbon chain. Similarly, the constrained end-to-end distance of the hydrocarbon chain was also maintained via this procedure. The time step was set to 2.0 fs. Room temperature was maintained by periodically rescaling the velocities. All interactions were spherically truncated at 9.3 Å. The simulations were carried out with a constant volume resulting in equilibrium pressures in the range ±100 atm for the studied systems.

A set of 100 simulations with end-to-end separations, r_{ee}, between 14.0 and 4.0 Å was carried out to characterize the free-energy change according to Eq. 6 and Eq. 7 for each solvent. A separation of 14.0 Å characterizes the fully extended all-*trans* conformation and serves as the overall reference state, whereas 4.0 Å is the turning point of the LJ interaction between two end CH_3 units. The distance r_{ee} was uniformly changed in steps of 0.1 Å for the reference states, and the free-energy changes were accumulated for each reference state. Thermodynamic averages were then calculated from block averaging five simulations of 10.0 ps each. The error of the free energy for the perturbed systems was estimated as twice the standard deviation obtained from block averaging. As the perturbation technique estimates the change in free energy relative to each reference system simulated, the total free-energy change is reconstructed by connecting the individual free-energy curves from each reference system.

The calculations of the free-energy change for the LJ water and the CCl_4 solvents required approximately 900 cpu h on a DEC-alpha model 3000/800 workstation.

RESULTS AND DISCUSSION

Solvent characteristics

The difference between water and Lennard-Jones liquid structures is highlighted in the pair distribution function of solvent molecules in Fig. 1. The RER(pair) water model exhibits the typical hydrogen bonding pattern in water, characterized by the tetrahedrally positioned next-nearest-neighbor peak at $r \approx 4.5$ Å, or $r \approx 1.6\sigma$, where σ is the hard-sphere radius of water. This is commensurate with each water having, on average, four nearest neighbors arranged in a tetrahedron around a central water. Although the first peak, corresponding to nearest neighbors at 2.9 Å, coincides for the LJ water and the RER(pair) water, by construction, the position of the more distant peaks differs because of lack of the tetrahedral coordination in the LJ fluid. The LJ water, as well as the CCl_4 liquid, is consistent with a simple solvent structure where the second peak is situated at $r \approx 2\sigma$. Although the LJ waters lack a directional hydrogen bond pattern, the "size" of a molecule in this fluid is the same as that of the RER(pair) water, making this model a "first-order" approximation to a liquid water model.

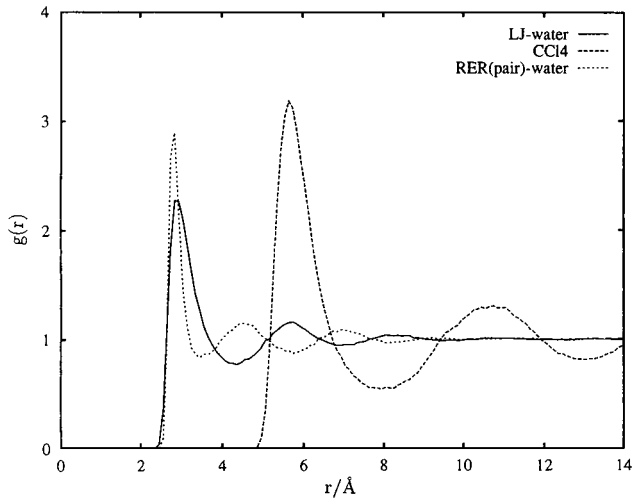

FIGURE 1 Pair distribution functions of the liquid solvents used in this study. Note the similarity in size between the RER(pair) water and the single-site LJ water model. For the RER water model the radial distribution function of oxygen pairs is given. The structural correlation for the water fluid dies out after $r \approx 10$ Å or about 3σ.

The difference between the RER(pair) and LJ-water potential function lies in the much stronger interactions that can be developed between RER(pair) molecules as compared to the nonpolar LJ water. Whereas the weak interactions of the LJ potential are of a dispersive nature, water is characterized by dipolar forces. In the RER(pair) model these forces are derived from a set of partial charges that are arranged to give a fixed dipole moment. A LJ liquid of the same size, with the same strength of the dimer interaction, would rapidly freeze at standard temperature and pressure. Thus dipolar forces, or hydrogen bonds, are the primary reason that the strongly interacting water molecules can maintain a liquid phase of 1.0 g/cc at 300 K and 1 atm.

On the other hand, the primary difference between the LJ water and the CCl_4 liquid is the size of the individual molecules. A carbon tetrachloride molecule occupies a volume almost eight times as large as that of a LJ water molecule. Macroscopically there is a large difference between water and CCl_4 surface tension coefficients: whereas water/vapor has an interfacial surface tension of 72 dyn/cm, the carbon tetrachloride/vapor interfacial value is only 27 dyn/cm (Weast, 1986). The lack of cohesiveness of the liquid CCl_4 phase is also reflected in its boiling point of 350 K, as compared to 373 K for water (Weast, 1986). From a macroscopic point of view it should then be easier to maintain, as well as distort, solute-occupied cavities in the CCl_4 liquid phase when compared to water. Even though it is tempting to translate this picture to the formation of microscopic cavities of the same size as solvent and solute molecules, there is no theoretical ground for doing so (Ben-Naim and Mazo, 1993; Ben-Naim, 1994). Accordingly, efforts to find an empirical connection between free-energy costs of cavity formation in molecular liquids and the surface tension have not been successful (Pohorille and Pratt, 1990; Pratt and Pohorille, 1992; Wallqvist and Berne, 1995a,b; Wallqvist and Covell, 1995).

Perturbation path

Although the procedure for calculating the free-energy change was shown to be adequate for the gas phase (Wallqvist and Covell, 1995), the same need not be true for a condensed phase. As a further check on the validity of the procedure, we monitored the radius of gyration as a function of end-to-end distance for the various conformations generated. Thus, a radius of gyration, r_g, was calculated from the mass-weighted average distance from the center of mass, $\mathbf{r}_{com}$, as

$$r_g = \frac{1}{M} \sum_{i=1}^{N} \mid m_i(\mathbf{r}_i - \mathbf{r}_{com}) \mid , \qquad (8)$$

where m_i is the mass of the united atom and M is the total mass of the molecule. In Fig. 2 we compare the most probable values of r_g as a function of r_{ee} for the gas phase and the liquid phase simulations. There is general agreement among all systems, indicating that we are following the same perturbation in all systems and thus we can compare the free-energy changes associated with the distortion of the *n*-dodecane molecule.

Snapshots of the hydrocarbon chain conformation taken from the simulations show that this perturbation path takes the fully extended molecule and contorts it into its most compact form, a hairpin bend, characterized by $r_{ee} = 4.0$ Å and $\langle r_g \rangle = 2.7$ Å. In Fig. 3 two configurations are shown, which correspond to an extended and a compact state.

Free-energy considerations

Fig. 4 plots the free-energy map of the transition between extended states and the collapsed conformation following

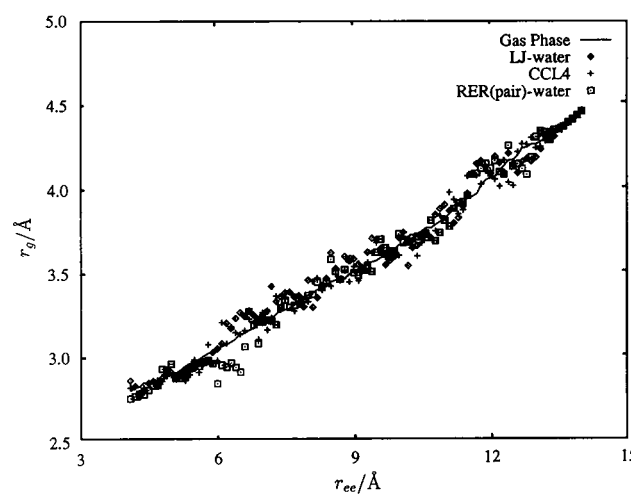

FIGURE 2 The radius of gyration, r_g, of the *n*-dodecane molecule as a function of end-to-end distance, r_{ee}, in various media. All simulations of the hydrocarbon molecule in condensed media follow the same perturbation path as in the gas phase.

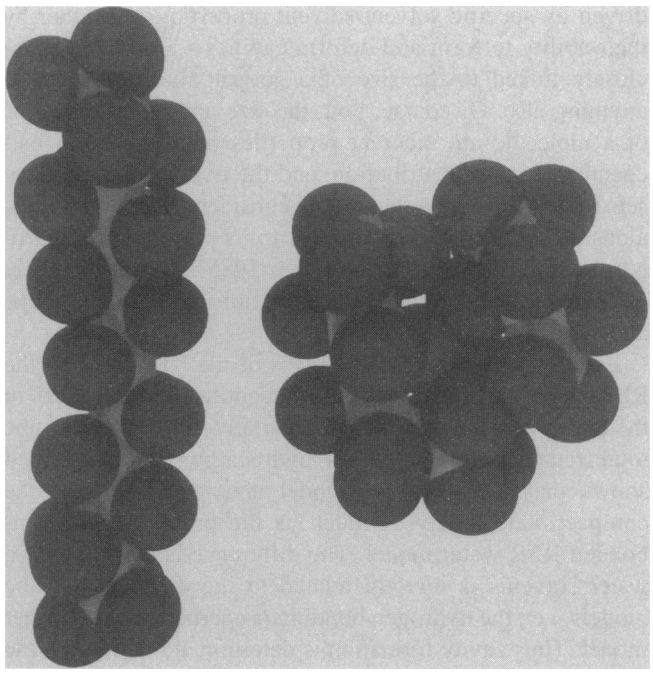

FIGURE 3 Two *n*-dodecane conformations corresponding to an extended and a compact chain. The hydrogen atoms are added for artistic effect, although it is clear from the occupied volume that the compact chain has formed a hydrophobic region that is inaccessible to the solvent.

the perturbation path in Fig. 2 in various solvents. As the most probable set of conformations for the dodecane molecule in all phases corresponds to extended configurations, we have anchored the free-energy changes to this region between $10 < r_{ee}/\text{Å} < 13$ by adjusting the curves to the same average energy in this range. It is only the RER(pair) water solvent that has a pronounced effect on the compact states, lowering them by 8 kJ/mol of free energy. None of the LJ solvents show such a large stabilizing effect, although the LJ water is clearly imparting an added stability to the states in the range $r_{ee}/\text{Å} < 6$ compared with the CCl_4 solution. Conversely, the extended forms of the *n*-dodecane molecule are strongly favored by the CCl_4 solution.

The enthalpy and entropy contributions from the solvent part of the system can be separated by forming the differences

$$\Delta\Delta H \equiv \Delta H_{\text{sol}} - \Delta H_{\text{gas}} \tag{9}$$

$$-T\Delta\Delta S \equiv -T(\Delta S_{\text{sol}} - \Delta S_{\text{gas}}), \tag{10}$$

where the enthalpic and entropic values in the solution (sol) and gas-phase (gas) have been calculated using Eqs. 6 and 7. The resulting $\Delta\Delta$ quantities contain the solvent response as well as the terms arising from the coupling of the solute to the solvent bath. In Fig. 5 these components of the free energy are seen to be largely compensating each other, regardless of solvent. The enthalpy change going from the extended state to the compact state is positive, i.e., the compact state is disfavored from energetic considerations. As solute-solvent contacts are diminished in the interface during contraction, van der Waals attractions between solute-solvent pairs in the interface are simultaneously reduced. Additionally released solvent molecules from the interface are incorporated into the surrounding bulk phase. The RER(pair) water and LJ water liquids have a similar qualitative behavior, indicating that for most of the configurations it is the solvent-solute contacts that are the determining factor in the enthalpic change. Even though the solvent-solvent energy is different for these two fluids, in the systems studied here these energy changes are closely maintained regardless of the shape of the hydrocarbon chain. Thus, real water is characterized by strong directional hydrogen bond forces that appear to be less important than the generic solvent/solute interaction lost through shrinking of the solvent/solute interface. In the CCl_4 solution the same trends are visible for the enthalpy change, yet their magnitude is much less than for the equal-sized water solvents.

Folding the hydrocarbon chain from extended states to compact states results in lower free energy in terms of $-T\Delta\Delta S$. The positive nature of $\Delta\Delta S$ indicates that the entropy penalties for the solvent in the compact state are less than in the extended water cavity containing the *n*-dodecane molecule. This is a direct consequence of releasing "constrained" solvent molecules into the bulk solvent, where "constrained" is meant to indicate thermodynamic states unlike those in the bulk liquid. These entropy changes are opposite to those of enthalpy, again with a perceivable similarity between the two model water fluids. In this case the difference between the LJ and RER water is more pronounced than for the enthalpic changes. The entropic response of the CCl_4 solution to the deformation of the dodecane molecule is clearly distinct from the water models.

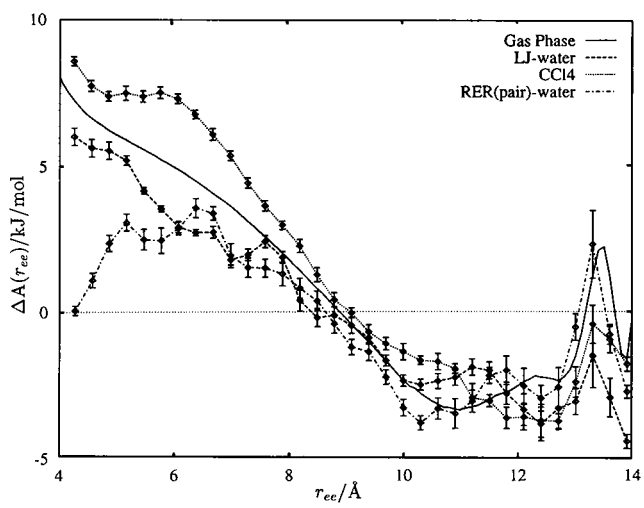

FIGURE 4 The Helmholtz free-energy change of the *n*-dodecane/solvent system as a function of the end-to-end distance, r_{ee}. Extended conformations of the hydrocarbon chain are the most stable molecular arrangements in all solvents investigated. Although the calculation of the free energy changes in Eq. 6 relate only to differences, the absolute values of the free energy cannot be compared between the solvents at any given r_{ee}.

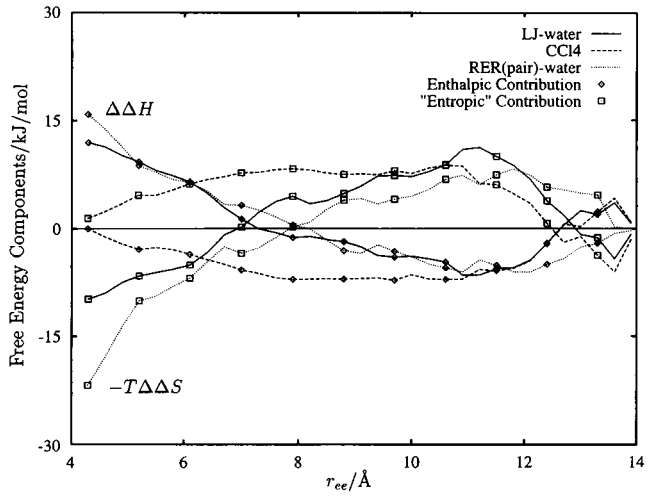

FIGURE 5 Decomposition of the free energy into enthalpic $\Delta\Delta H$ and entropic $-T\Delta\Delta S$ solvent contributions. The opposing natures of these components are evident; the resultant total free-energy sum in Fig. 3 is much smaller in magnitude than the individual constituent parts.

The compact cavity does have a higher entropy ($-T\Delta\Delta S$ is lower) compared to the most probable extended states ($10 < r_{ee}/\text{Å} < 13$) for all of the solvent systems studied here. The difference is smallest for the CCl_4 solvent, and it is significantly larger for both water solvents, with the hydrogen-bonded (RER) water exhibiting the largest effect. Generally a smaller cavity is entropically favored over a large cavity because of the reduction of exposed solvent molecules at the interface (i.e., fewer solvent molecules need to arrange themselves to accommodate the cavity). As the cavities studied in this work are greater than naturally occurring voids in these solvents, the cavity shapes are intimately connected with the volume and volume fluctuations of the *n*-dodecane molecule. As the solvent size increases, the entropic response, as measured in Fig. 5, indicates that the solvent becomes less sensitive to the size of the solute.

Although there is a qualitative similarity between the water-like LJ solvent and the hydrogen-bonded water solvent, the simplified solvent cannot quantitatively account for real water behavior. The entropy change ($-T\Delta\Delta S$) from a compact to a most probable extended state is ~5 kJ/mol for the CCl_4 solvent, ~20 kJ/mol for LJ water and ~30 kJ/mol for the hydrogen-bonded RER water. Thus the "size" contribution accounts for two-thirds of the total entropic response.

A qualitative correspondence in the entropy/enthalpy compensation is also exhibited for the CCl_4 solution, although the magnitudes are not comparable to the water-sized liquids. Although a lowering of the free energy from the $-T\Delta S$ contribution for aqueous solvents has often been interpreted in terms of solvent ordering, the similarity between the LJ and the RER water is not in accord with such an interpretation, at least in terms of specific hydrogen-bonded assemblies. The changes in entropy appear not to be driven by specific solvent-solvent properties, but rather by their ability to form and deform cavities—a property more closely linked to the size of a solvent molecule than to anything else. Of course, both the size and the interactions of a molecule are inherent properties of its quantum mechanical electron distribution, and the two concepts are not separable—except in theoretical considerations. The anomalous properties of water are due to its size, not the hydrogen-bonded network per se (Lee, 1985; Madan and Lee, 1994), except in terms of the interactions defining the shape and size of the molecule.

Even if the free-energy changes of the LJ water and the RER water are similar, there are quantitative differences in the entropy change leading to qualitative differences in the total free-energy profile of the hydrocarbon collapse. Fig. 4 shows that the LJ water model does not influence the compact state nearly as much as the properly hydrogen-bonded RER water model. The difference between the two water solvents is directly related to the difference in the models, i.e., the hydrogen bonding properties of a real water model. Thus cavity formation is determined not only by the size of the solvent; also of importance is the means (hydrogen bonding) by which water realizes its structure around solutes and in solution. This difference between the water systems is exhibited in the entropic contributions and is shown in Fig. 6. Here we have subtracted the LJ water part, arising from translations of the spherically symmetric water molecules, from the water solvent entropy change as

$$-T\delta S \equiv -T(\Delta\Delta S_{H_2O(RER)} - \Delta\Delta S_{H_2O(LJ)}). \quad (11)$$

This quantity will then contain the rotational contribution not present in a same-sized spherical solvent as well as any difference in packing due to anisotropies of the hydrogen-bonded water molecules. Again, these differences are a

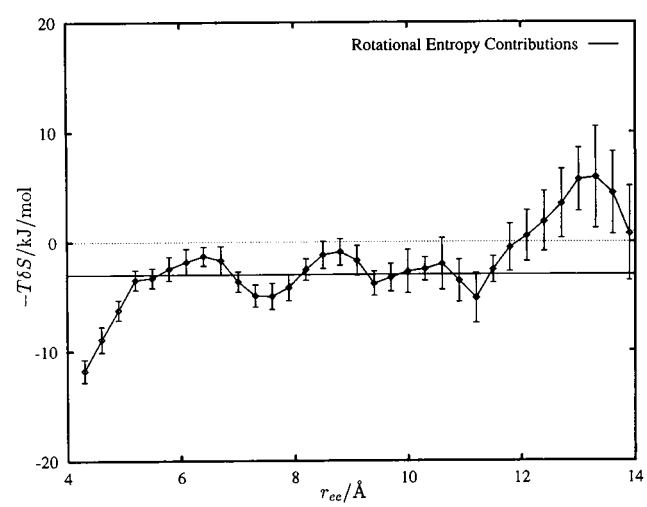

FIGURE 6 Water solvent excess entropy after subtracting the translational contributions of the simplified water model. Nominally this excess entropy should correspond to the rotational contributions present in the more elaborate RER parameterization of intermolecular water-water interactions, including explicit hydrogen atoms.

direct consequence of the hydrogen bonding capabilities included in the RER water potential, but left out in the LJ water model. Although an identification of this quantity with the rotational part of the entropy change is tentative, it does highlight the main differences between the two water-like solvents. In the region between $6 < r_{ee}/\text{Å} < 11$ there is a roughly constant difference, indicating that the rotational part is constant over this range of hydrocarbon collapse. There are, however, strong deviations for both extended and compact states, resulting from different rotational constrictions associated with these water cavities. Theoretical considerations by Lazaridis and Paulaitis (1992, 1994) of the entropic contributions to the hydrophobic solvation of methane and rare gas atoms in water indicate that 40% to 50% of this quantity arises from rotational effects. Although our data cannot be directly applied to such a system, it is clear that rotational effects are strongly dependent on the shape of the solvent cage and can approach such magnitudes for specific cases.

CONCLUSIONS

Each solvent considered here must form a cavity to accommodate an *n*-dodecane molecule. This cavity is deformed and contracted as the *n*-dodecane molecule is forced to bend on itself in our calculations. The entropic solvent component for this process is attractive and is partially balanced by the enthalpy changes, depending on the solvent. It is true that entropy is a measure of order and disorder, but this consideration follows from arguments about the number of microstates available to a system in a specified thermodynamic state. Thus the favorable free-energy change of water in reducing the solute-exposed cavity is ultimately derived from an increased number of solvent microstates associated with the smaller cavities. This entropic phenomenon has no simple analog in terms of number of hydrogen bond interactions or specific clathrate structures. For the "real" water model considered here, solvent contributions stabilize the compact state, but not enough to make these hydrocarbon states the most probable ones in solution. For larger chains or for more concentrated alkane solutions, we know that for a macroscopic as well as microscopic system (Wallqvist, 1991) there is an aggregation and phase separation of alkanes and water. Given the small magnitude of the solvent-induced hydrophobic attraction per solvent molecule calculated here, the observation of hydrophobicity in model simulations requires very large systems. This makes molecular model studies of the free-energy profile of hydrophobic association in macromolecular system very challenging.

As was shown by Pratt and Pohorille (1992), a major difference in the molecular behavior of water and hydrocarbon liquids is the distribution of free volumes in the fluid. The larger the naturally occurring volume fluctuations are, the more likely an expansion or deformation of a cavity in a fluid will be, i.e., it will cost less in free energy to expand or do work against such a solvent-fluid interface. Likewise, the gain in free energy needed to contract a cavity in such a fluid is greater. These volume fluctuations depend largely on the size of the involved molecules, not on the nature of the intermolecular forces determining their size. The resultant free-energy behavior of such aqueous solvents is in accord with the simulation data presented in this paper. This work indicates that a hydrogen-bonded water model as well as a simplified LJ model have a qualitatively similar free-energy response in terms of enthalpic and entropic solvent contributions. The important quantitative differences in their free-energy response is directly related to the treatment of hydrogen bonds in these solvents. On the other hand, a prototype LJ liquid modeled after CCl_4 has a qualitatively different and distinct free-energy response to the deformation of an *n*-dodecane molecule. Because the entropic part of the free energy is similar for the two water models, our results suggest that it must be their common feature—size—that is responsible for this similarity.

Special thanks are extended to Dr. S. Durell for valuable comments regarding the manuscript. The staff of the Biomedical Supercomputing Center, FCRDC, Frederick, MD, is thanked for its assistance and for access to its computer facilities.

This research is sponsored by the National Cancer Institute, Department of Health and Human Services (DHHS), under contract with Science Applications International Corporation. The contents of this publication do not necessarily reflect the views or policies of the DHHS, nor does mention of trade names, commercial products, or organizations imply endorsement by the U.S. Government.

REFERENCES

Andersen, H. C. 1983. Rattle: a "velocity" version of the shake algorithm for molecular dynamics calculations. *J. Comput. Phys.* 52:24–34.

Ben-Naim, A. 1974. Water and Aqueous Solutions. Plenum, New York.

Ben-Naim, A. 1994. Solvation: from small to macro molecules. *Curr. Opin. Struct. Biol.* 4:264–268.

Ben-Naim, A., and R. M. Mazo. 1993. Size dependence of the solvation free energies of large solutes. *J. Phys. Chem.* 97:10829–10834.

Berendsen, H. J. C., J. R. Grigera, and T. P. Straatsma. 1987. The missing term in effective pair potentials. *J. Phys. Chem.* 91:6269–6271.

Beveridge, D. L., and F. M. DiCapua. 1989. Free energy via molecular simulations: applications to chemical and biomolecular systems. *Annu. Rev. Biophys. Biophys. Chem.* 18:431–492.

Blokzijl, W., and J. B. F. N. Engberts. 1993. Hydrophobic effects. Opinions and facts. *Angew. Chem. Int. Ed. Engl.* 32:1545–1579.

Chan, D. Y. C., D. J. Mitchell, B. W. Ninham, and B. A. Pailthorpe. 1979. Solvent structure and hydrophobic solutions. *In* Water: A Comprehensive Treatise, Vol. 6. F. Franks, editor. Plenum, New York. 239–278.

Crovetto, R., R. Fernandez-Prini, and M. L. Japas. 1982. Solubilities of inert gases and methane in h_2o and in d_2o in the temperature range of 300 to 600 K. *J. Chem. Phys.* 78:1077–1086.

Dill, K. A. 1990. Dominant forces in protein folding. *Biochemistry.* 29: 7133–7155.

Eley, D. D. 1939a. On the solubility of gases. Part I. The inert gases in water. *Trans. Faraday Soc.* 35:1281–1293.

Eley, D. D. 1939b. On the solubility of gases. Part II. A comparison of organic solvents with water. *Trans. Faraday Soc.* 35:1421–1432.

Franks, F. 1975. The hydrophobic interaction. *In* Water: A Comprehensive Treatise, Vol. 4. F. Franks, editor. Plenum, New York. 1–94.

Harris, J. G. 1992. Liquid-vapor interface of alkane oligomers. Structure and thermodynamics from molecular dynamics simulations of chemically realistic models. *J. Phys. Chem.* 96:5077–5086.

Holtzer, A., and M. F. Emerson. 1969. On the utility of the concept of water structure in the rationalization of the properties of aqueous solutions of proteins and small molecules. *J. Phys. Chem.* 73:26–33.

Jorgensen, W. L. 1982. Monte Carlo simulation of *n*-butane in water. Conformational evidence for the hydrophobic effect. *J. Chem. Phys.* 77:5757–5765.

Jorgensen, W. L., J. D. Madura, and C. J. Swenson. 1984. Optimized intermolecular potential functions for liquid hydrocarbons. *J. Am. Chem. Soc.* 106:6638–6646.

Kauzmann, W. 1959. Some factors in the interpretation of protein denaturation. *Adv. Protein Chem.* 14:1–63.

Lazaridis, T., M. E. Paulaitis. 1992. Entropy of hydrophobic hydration: a new statistical mechanical formulation. *J. Phys. Chem.* 96:3847–3855.

Lazaridis, T., and M. E. Paulaitis. 1994. Simulation studies of the hydration entropy of simple, hydrophobic solutes. *J. Phys. Chem.* 98:635–642.

Lee, B. 1985. The physical origin of the low solubility of nonpolar solutes in water. *Biopolymers.* 24:813–823.

Leikin, S., V. A. Parsegian, D. C. Rau, and R. P. Rand. 1993. Hydration forces. *Annu. Rev. Phys. Chem.* 44:369–395.

Madan, B., and B. Lee. 1994. Role of hydrogen bonds in hydrophobicity: the free energy of cavity formation in water models with and without the hydrogen bonds. *Biophys. Chem.* 51:279–289.

New, M. H., and B. J. Berne. 1995. Molecular dynamics calculation of the effect of solvent polarizability on the hydrophobic interaction. *J. Am. Chem. Soc.* 117:7172–7179.

Pangali, C., M. Rao, and B. J. Berne. 1979a. A Monte Carlo simulation of the hydrophobic interaction. *J. Chem. Phys.* 71:2975–2981.

Pangali, C., M. Rao, and B. J. Berne. 1979b. Hydrophobic hydration around a pair of apolar species in water. *J. Chem. Phys.* 71:2982–2990.

Pohorille, A., and L. R. Pratt. 1990. Cavities in molecular liquids and the theory of hydrophobic solubilities. *J. Am. Chem. Soc.* 112:5066–5074.

Postma, J. P. M., H. J. C. Berendsen, and J. R. Haak. 1982. Thermodynamics of cavity formation in water. *Faraday Symp. Chem. Soc.* 17: 55–67.

Pratt, L. R., and D. Chandler. 1977. Theory of the hydrophobic effect. *J. Chem. Phys.* 67:3683–3704.

Pratt, L. R., and D. Chandler. 1980. Effects of solute-solvent attractive forces on hydrophobic correlations. *J. Chem. Phys.* 73:3434–3441.

Pratt, L. R., and A. Pohorille. 1992. Theory of hydrophobicity: transient cavities in molecular liquids. *Proc. Natl. Acad. Sci. USA.* 89:2995–2999.

Pratt, L. R., R. O. Rosenberg, B. J. Berne, and D. Chandler. 1980. Comment on the structure of a simple liquid solvent near a *n*-butane solute molecule. *J. Chem. Phys.* 73:1002–1003.

Rebertus, D. W., B. J. Berne, and D. Chandler. 1979. A molecular dynamics and Monte Carlo study of solvent effect on the conformational equilibrium of *n*-butane in CCl_4. *J. Chem. Phys.* 70:3395–3400.

Reiss, H. 1965. Scaled particle methods in the statistical thermodynamics of fluids. *Adv. Chem. Phys.* 9:1–84.

Rosenberg, R. O., R. Mikkilineni, and B. J. Berne. 1982. Hydrophobic effect on chain folding. The trans to gauche isomerization of *n*-butane in water. *J. Am. Chem. Soc.* 104:7647–7649.

Sloan, E. D. 1990. Clathrate Hydrates of Natural Gases. Marcel Dekker, New York.

Smith, D. E., and A. D. J. Haymet. 1993. Free energy, entropy, and internal energy of hydrophobic interactions: computer simulations. *J. Chem. Phys.* 98:6445–6454.

Smith, D. E., L. Zhang, and A. D. J. Haymet. 1992. Entropy of association of methane in water: a new molecular dynamics computer simulation. *J. Am. Chem. Soc.* 114:5875–5876.

Stillinger, F. H. 1973. Structure in aqueous solutions of nonpolar solutes from the standpoint of scaled particle theory. *J. Solution Chem.* 2:141–158.

Swope, W. C., H. C. Andersen, P. H. Berens, and K. R. Wilson. 1982. A computer simulation method for the calculation of equilibrium constants for the formation of physical clusters of molecules: applications to small water clusters. *J. Chem. Phys.* 76:637–649.

Tanford, C. 1973. The Hydrophobic Effect. Wiley, New York.

Tobias, D. J., and C. L. I. Brooks. 1990. The thermodynamics of solvophobic effects: a molecular dynamics study of *n*-butane in carbon tetrachloride and water. *J. Chem. Phys.* 92:2582–2592.

Tsao, Y.-H., D. F. Evans, and H. Wennerström. 1993. Long-range attractive force between hydrophobic surfaces observed by atomic force microscopy. *Science.* 262:547–550.

Wallqvist, A. 1991. Molecular dynamics study of a hydrophobic aggregate in an aqueous solution of methane. *J. Phys. Chem.* 95:8921–8927.

Wallqvist, A., and B. J. Berne. 1993. Effective potentials for liquid water using polarizable and non-polarizable models. *J. Phys. Chem.* 97: 13841–13851.

Wallqvist, A., and B. J. Berne. 1995a. Molecular dynamics study of the dependence of water solvation free energy on solute curvature and surface area. *J. Phys. Chem.* 99:2885–2892.

Wallqvist, A., and B. J. Berne. 1995b. Computer simulation of hydrophobic hydration forces on stacked plates as short range. *J. Phys. Chem.* 99:2893–2899.

Wallqvist, A., and D. G. Covell. 1995. Free-energy cost of bending *n*-dodecane in aqueous solution. Influence of the hydrophobic effect and solvent exposed area. *J. Phys. Chem.* 99:13118–13125.

Watanabe, K., and M. L. Klein. 1989. Effective pair potentials and the properties of water. *Chem. Phys.* 131:157–167.

Weast, R. C., editor. 1985–1986. CRC Handbook of Chemistry and Physics, Vol. 66. CRC Press, Boca Raton.

Weiner, S. J., P. A. Kollman, D. A. Case, U. C. Singh, C. Ghio, G. Alagone, S. Profeta, and P. Weiner. 1984. A new force field for molecular mechanical simulation of nucleic acids and proteins. *J. Am. Chem. Soc.* 106:765–784.

Zichi, D. A., and P. J. Rossky. 1986. Molecular conformational equilibria in liquids. *J. Chem. Phys.* 84:1712–1723.